Research in Astron. Astrophys. **2010** Vol. **10** No. **2**, 116 – 124
http://www.raa-journal.org *http://www.iop.org/journals/raa*

***R**esearch in*
***A**stronomy and*
***A**strophysics*

Modeling the WMAP large-angle anomalies as an effect of a local density inhomogeneity

Li-Ping He[1,2] and Quan Guo[1]

[1] National Astronomical Observatories, Chinese Academy of Sciences, Beijing 100012, China; *hlp@bao.ac.cn*
[2] Graduate University of Chinese Academy of Sciences, Beijing 100049, China

Received 2009 April 18; accepted 2009 December 7

Abstract We investigate large-angle scale temperature anisotropy in the Cosmic Microwave Background (CMB) with the Wilkinson Microwave Anisotropy Probe (WMAP) data and model the large-angle anomalies as the effect of the CMB quadrupole anisotropies caused by the local density inhomogeneities. The quadrupole caused by the local density inhomogeneities is different from the special relativity kinematic quadrupole. If the observer inhabits a strong inhomogeneous region, the local quadrupole should not be neglected. We calculate such local quadrupole under the assumption that there is a huge density fluctuation field in the direction $(284^\circ, 74^\circ)$, where the density fluctuation is 10^{-3}, and its center is $\sim 112\,h^{-1}\,\mathrm{Mpc}$ away from us. After removing such mock signals from WMAP data, the power in the quadrupole, C_2, increases from the range $(200 \sim 260\,\mu\mathrm{K}^2)$ to $\sim 1000\,\mu\mathrm{K}^2$. The quantity S, which is used to estimate the alignment between the quadrupole and the octopole, decreases from $(0.7 \sim 0.74)$ to $(0.31 \sim 0.37)$, while the model predicts that $C_2 = 1071.5\,\mu\mathrm{K}^2$, and $S = 0.412$. So our local density inhomogeneity model can, in part, explain the WMAP low-ℓ anomalies.

Key words: cosmology: cosmic microwave background — cosmology: large-scale structure of universe

1 INTRODUCTION

Although the WMAP data are regarded as a dramatic confirmation of standard inflationary cosmology (Vale 2005; de Oliveira-Costa & Tegmark 2006; Gaztañaga et al. 2003; Gordon et al. 2005), some anomalous features have emerged (Inoue & Silk 2006; Campanelli et al. 2006; Schwarz et al. 2004). Firstly, the amplitude of the quadrupole is substantially less than the expectation from the best-fit $\Lambda\mathrm{CDM}$ standard model (Abramo et al. 2006; de Oliveira-Costa et al. 2004; Efstathiou 2004), which was found by COBE a decade ago (Bennett et al. 1996) and confirmed by WMAP (Spergel et al. 2003). Secondly, the quadrupole and octopole indicate an unexpectedly high degree of alignment (Spergel et al. 2003; de Oliveira-Costa et al. 2004, de Oliveira-Costa & Tegmark 2006; Schwarz et al. 2004; Land & Magueijo 2005; Hansen et al. 2004a; Eriksen et al. 2004).

Recently, many efforts have been devoted to explaining the origin of the anomalies. They can be systematic errors, statistical flukes, the improper subtraction of known foreground, or an unexpected

foreground (Copi et al. 2004, 2006, 2007). The WMAP team claims that there are no unexpected systematic errors (Bennett et al. 2003; Finkbeiner 2004), and Copi et al. (2004, 2006, 2007) noted that the anomalies are very unlikely to be due to residual foreground contamination. Several authors attempted to explain the anomalies in terms of a new foreground (Abramo et al. 2006; Gordon et al. 2005; Bennett et al. 2003; Finkbeiner 2004; Prunet et al. 2005; Rakic et al. 2006).

Abramo et al. (2006) showed circumstantial evidence that an extended foreground near the dipole axis could distort the CMB. They proposed that the possible physical mechanism, which can produce such a foreground, is the thermal Sunyaev-Zeldovich (SZ) effect. However, the SZ model, as presented by them, cannot successfully account for the anomalous quadrupole and octopole. Therefore, they thought that the Ress-Sciama (RS) effect (Rakic et al. 2006), or the combination of SZ effect and RS effect may be responsible for the foreground. Many other authors suggested that the large-angle anomalies are affected by local inhomogeneities (Tomita 2005a,b; Vale 2005). However, when they applied a model in which the Local Group is falling into the center of the Shapley supercluster, the discrepancy between the observed data and the model prediction became even worse. (Rakic et al. 2006; Inoue & Silk 2007).

Inoue & Silk (2007) explored the large angular scale temperature anisotropies due to homogeneous local dust-filled voids in a flat Friedmann-Robertson-Walker universe. They found that a pair of voids with radius $(2 \sim 3) \times 10^2\, h^{-1}\,\mathrm{Mpc}$ and density contrast $\delta_m \sim 0.3$ might help explain the observed large-angle CMB anomalies. Concurrently, Wu & Fang (1994) explored the possibility that the CMB is affected by local density inhomogeneities based on the Tolman-Bondi model. They calculated the quadrupole amplitude of the local collapse model with general relativity (GR). The results show that the CMB anisotropies from the local quadrupole contribution can be different from the special relativity (SR) kinematic quadrupole by a factor as large as 3, which depends on the size and density fluctuation of the region the observer inhabits. Therefore, if we live in a large density fluctuation area, the local quadrupole might be significant in the CMB observations.

The goal of this paper is to examine whether such a local quadruple could account for the observed large-angle CMB anomalies in WMAP data. Our analysis is based on the 1-year, 3-year and 5-year WMAP Internal Linear Combination maps (Spergel et al. 2006; Hinshaw et al. 2006) (henceforth ILC1, ILC3 and ILC5). We try to remove the mock CMB foreground caused by the effect described in Wu & Fang (1994) for each observed CMB map under the assumption that we are in a huge density fluctuation area. The parameters of the area we adopted are based on Kocevski & Ebeling (2006) and Watkins et al. (2009)'s work. We reanalyze the WMAP data by using the multipole vector framework in Section 2. In Section 3, we review the estimate of the foreground of Wu & Fang (1994) and present the result of our examination. We conclude in Section 4.

2 LARGE-ANGLE ANOMALIES OF CMB

In this section, we re-investigate the anomalies reported from the WMAP maps on a very large angular scale. As we already remarked, the angular power in the quadrupole, C_2, is less than expected. To measure C_2, we expand the temperature anisotropy in terms of spherical harmonics (Campanelli et al. 2006; Copi et al. 2004)

$$\Delta T(\theta, \phi) = \sum_{\ell=1}^{\infty} \sum_{m=-\ell}^{\ell} a_{\ell m} Y_{\ell m}(\theta, \phi). \tag{1}$$

Also, the angular power spectrum is defined as

$$C_\ell \equiv \frac{1}{2\ell + 1} \sum_{m=-\ell}^{\ell} |a_{\ell m}|^2. \tag{2}$$

Table 1 Power in quadrupole C_2 and alignments of the CMB maps for ILC1, ILC3 and ILC5. The final row shows the expected power in the quadrupole and the average value of S statistics of the 10^6 Gaussian random statistically isotropic CMB maps. $P(S)$ is the probability that a random map has a quadrupole-octopole alignment as high as S.

	$C_2\,(\mu\mathrm{K}^2)$	S	$P(S)\,(\%)$
ILC1	204.4	0.744	0.8
ILC3	260.3	0.700	2.1
ILC5	254.1	0.726	1.2
ΛCDM	1071.5	0.412	50.0

A simple way to quantify the peculiar alignment of the quadrupole and octopole is to use the multipole vectors. In the multipole vector representation, the ℓ-th multipole of the CMB, T_ℓ, can be written in terms of a scalar $A^{(\ell)}$ and ℓ unit vectors $\{\hat{v}^{(\ell,i)}|i=1,\cdots,\ell\}$ (Schwarz et al. 2004; Copi et al. 2006, 2007)

$$T_\ell \approx A^{(\ell)} \prod_{i=1}^{\ell} (\hat{v}^{(\ell,i)} \cdot \hat{e}). \tag{3}$$

For the statistical comparison, we use the area vectors

$$\boldsymbol{w}^{(\ell;i,j)} \equiv \hat{v}^{(\ell,i)} \times \hat{v}^{(\ell,j)}. \tag{4}$$

The alignments between the quadrupole area vector and the three octopole area vectors can be evaluated by the magnitudes of the dot products between $\boldsymbol{w}^{(2;1,2)}$ and each $\boldsymbol{w}^{(3;i,j)}$

$$\begin{aligned} A_1 &\equiv |\boldsymbol{w}^{(2;1,2)} \cdot \boldsymbol{w}^{(3;1,2)}| \\ A_2 &\equiv |\boldsymbol{w}^{(2;1,2)} \cdot \boldsymbol{w}^{(3;2,3)}| \\ A_3 &\equiv |\boldsymbol{w}^{(2;1,2)} \cdot \boldsymbol{w}^{(3;3,1)}|. \end{aligned} \tag{5}$$

The widely used estimator that checks for alignments of the quadrupole and octopole planes is the average of the dot products (Abramo et al. 2006; Katz & Weeks 2004; Schwarz et al. 2004)

$$S = \frac{1}{3} \sum_{i=1}^{3} A_i. \tag{6}$$

Given a CMB map, the harmonic components can be easily extracted with the HEALPix [1] (Górski et al. 2005) software, and the multipole vectors can be calculated by the code provided by Copi et al. (2004). Our analysis is based on the 1-year, 3-year and 5-year WMAP full sky maps (ILC1, ILC3, ILC5). The values of C_2 and S for ILC1, ILC3 and ILC5 are listed in Table 1. We can see that C_2 lies in the range $(200 \sim 260\,\mu\mathrm{K}^2)$.

In order to compare with the ΛCDM standard model, 10^6 mimic CMB maps are generated with Monte Carlos (MC) simulations based on theoretical CMB power spectra predicted by the ΛCDM model, which is generated by the CAMB [2] (Lewis et al. 2000) package with the best-fitting cosmological parameters estimated from WMAP (Hinshaw et al. 2009). In the ΛCDM model, the power in the quadrupole is $C_2 = 1071.5\,\mu\mathrm{K}^2$, while the power in the quadrupole for the ILC1, ILC3 and ILC5 are $C_2 = 204.4\,\mu\mathrm{K}^2$, $C_2 = 260.3\,\mu\mathrm{K}^2$, and $C_2 = 254.1\,\mu\mathrm{K}^2$ respectively. Clearly, the WMAP data have a low power in quadrupole compared to the ΛCDM model.

[1] *http://healpix.jpl.nasa.gov/*

[2] *http://camb.info/*

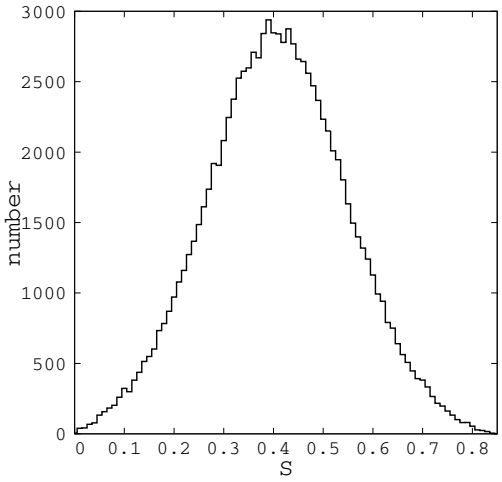

Fig. 1 Histogram of S statistics for 10^6 Gaussian random, statistically isotropic Monte Carlo maps.

Figure 1 is the histogram of the S statistics generated from 10^6 Gaussian random, statistically isotropic MC mock maps. The average value of S from 10^6 MC simulations is $S_{\Lambda\mathrm{CDM}} = 0.412$, which is much lower than the S statistics from WMAP data, which is $S = 0.744$ for ILC1, $S = 0.700$ for ILC3, and $S = 0.726$ for ILC5. The final rank in Table 1 lists the odds $P(S_{\Lambda\mathrm{CDM}} > S)$ of finding a value among the 10^6 MC maps larger than the one observed, from which one can see that the probabilities are 0.8% for ILC1, 2.1% for ILC3, and 1.2% for ILC5. This means that the alignment between quadrupole and octopole for each WMAP map is significant.

These alignments could be explained by an unexpected foreground caused by a local collapse due to the second-order effect of the density fluctuation area (Wu & Fang 1994). In next section, we will briefly discuss this foreground.

3 HYPOTHETICAL FOREGROUND INDUCED BY SUPER LARGE STRUCTURE

The CMB temperature anisotropy produced by a local spherical collapse can be modeled based on a Tolman-Bondi universe solution (Wu & Fang 1994).

Because we are interested in the effect of a local density fluctuation, in the following we only consider the case of $X_0 < X_c$, where $X_0 = x_0/t_e$, x_0 is the distance between the observer and the center of the perturbation, $X_c = x_c/t_e$, where x_c is the size of the perturbed region. When the initial density perturbation δ_0 is assumed to be constant in the region $x \leq x_c$, the first-order solution of the $\Delta\mathsf{T}/\mathsf{T}$, which is the CMB anisotropy produced by the local collapse, consists mainly of two parts: a monopole term and a dipole term which we are familiar with. The second-order solution of $\Delta\mathsf{T}/\mathsf{T}$ is (Wu & Fang 1994)

$$\frac{\Delta\mathsf{T}}{\mathsf{T}} = \delta_0^2\left[\left(\frac{3}{175}X_c^2 - \frac{11}{1575}X_0^2\right)T_0^{2/3} + \frac{4}{175}T_0 X_0\cos\Psi + \frac{2}{225}T_0^{2/3}X_0^2\cos 2\Psi\right], \qquad (7)$$

where $T_0 = (1+z_{\mathrm{d}})^{3/2}$ and z_{d} is the redshift at decoupling time t_e, and Ψ is the incidence angle of the photon.

When the terms of the order of δ_0^2 and $T_0^{1/3}$ are taken into account, the quadrupole anisotropy caused by local density fluctuation should be (Wu & Fang 1994)

$$\left(\frac{\Delta \mathsf{T}}{\mathsf{T}}\right)_q = \frac{2}{225} T_0^{2/3} X_0^2 \delta_0^2 \cos 2\Psi + T_0^{1/3} X_0^2 \Delta_q \delta_0^2, \tag{8}$$

and

$$\begin{aligned}\Delta_q \;=\; & -\frac{19X_c}{3780} - \frac{1}{X_0}\left(\frac{X_0}{140X_c} + \frac{229X_0^3}{61440X_c^3} + \frac{261X_0^5}{81920X_c^5} + \frac{3X_0^7}{4096X_c^7}\right) \\ & + X_0\left[\frac{41X_0}{9800X_c} - \frac{1333X_0^3}{2064384X_c^3} + \frac{467X_0^5}{5734400X_c^5} + \frac{3833X_0^7}{11468800X_c^7} + O\left(\frac{X_0^9}{X_c^9}\right)\right]. \end{aligned} \tag{9}$$

The first term on the left-hand side of Equation (8) is the SR kinematic quadrupole anisotropy. Equation (8) tells us that if higher orders are involved, the SR kinematic quadrupole may not always be a good approximation of the quadrupole produced by a local collapse. The local quadrupole anisotropy strongly depends on the size, the matter density in the peculiar field, and the position of the observer. Figure 2 shows the quadrupole amplitude as a function of the distance between the observer and the local gravitational field x_0. The SR kinematic quadrupole is denoted by the solid curve, and the local quadrupole is denoted by the dotted curve. We assume $x_c = 1000\,h^{-1}\,\mathrm{Mpc}$ to satisfy $x_c > x_0$. The quadrupole shown in Figure 2 is along the center of the perturbation. Figure 3 shows the relationship between the amplitude of the local quadrupole and the radius of the local gravitational field x_c for $x_0 = 112\,h^{-1}\,\mathrm{Mpc}$. In this case, x_c changes from $150\,h^{-1}\,\mathrm{Mpc}$ to $1000\,h^{-1}\,\mathrm{Mpc}$. Because the distance of the observer to the center of the collapse should at least be greater than the distance to the Great Attractor, which is estimated to be $80\,h_{50}^{-1}\,\mathrm{Mpc}$. Therefore, it would be reasonable to take the lower value of $x_c = 150\,h^{-1}\,\mathrm{Mpc}$ which is about 2 times the distance to the Great Attractor and the higher value of $x_c = 1000\,h^{-1}\,\mathrm{Mpc}$ which is about the size of the horizon (Wu & Fang 1994). We find that the influence of x_0 on the amplitude of the local quadrupole is about one magnitude larger than the influence of x_c. When x_0 is fixed, the results change little with x_c. Figure 4 shows the corrected C_2 of ILC5 as a function of x_c when $x_0 = 112\,h^{-1}\,\mathrm{Mpc}$. It turns out that $C_2 = 1022.3\,\mu\mathrm{K}^2$ for all values of x_c.

In order to explain the large-angle anomalies, we propose a model where we are in a large density fluctuation area. Kocevski & Ebeling (2006) suggest that 56% of the Local Group's (LG) peculiar velocity is induced by more distant overdensities between 130 and 180 Mpc away. Watkins et al. (2009) also note that the bulk flow within a Gaussian window of radius $50\,\mathrm{Mpc}$ is $407 \pm 81\,\mathrm{km\,s^{-1}}$ toward $l = 287^\circ \pm 9^\circ$, $b = 8^\circ \pm 6^\circ$, and roughly 50% of the LG's motion is due to sources at greater depths. Interestingly, we find that a region with a density fluctuation $\delta \sim 10^{-3}$ over a distance $\sim 112\,h^{-1}\mathrm{Mpc}$ away in the direction of $(284^\circ, 74^\circ)$ may be responsible for the origin of the anomalies over large angular scales. We compute the mock foreground (Eq. (8)) using these parameters. Figure 5 shows the map of the contribution of CMB anisotropies caused by the local density fluctuation.

After subtracting such a mock foreground from the CMB sky maps of the WMAP observation, we find that the power in quadrupole will dramatically increase and the alignment of the quadrupole and octopole plane will be weakened. In Table 2, we compare the quadrupole and S obtained from the "foreground-corrected" WMAP data to those obtained from the fiducial ΛCDM model. The powers in quadrupole of the three WMAP maps increase to $C_2 = 1064.2\,\mu\mathrm{K}^2$, $C_2 = 1034.2\,\mu\mathrm{K}^2$, and $C_2 = 1022.3\,\mu\mathrm{K}^2$, respectively, which is apparently in much better agreement with the ΛCDM model. Furthermore, from the S statistics, one can see that the frequencies $P(S_{\Lambda\mathrm{CDM}} > S)$ of finding a ΛCDM simulation with an S value larger than that from WMAP seem to converge to 75.1% for ILC1, 61.5% for ILC3, and 62.2% for ILC5. Therefore, if such a large scale structure exists, the foreground model presented here cannot be neglected.

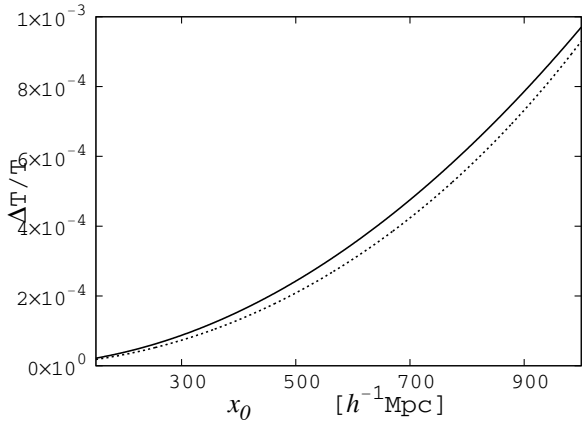

Fig. 2 Quadrupole amplitudes as a function of distance between the observer and local gravitational field. The solid line indicates the SR kinematic quadrupole, and the dotted line represents the local quadrupole. We assume a higher value for X_c, that is $x_c = 1000\,h^{-1}\,\mathrm{Mpc}$ to satisfy $X_0 < X_c$.

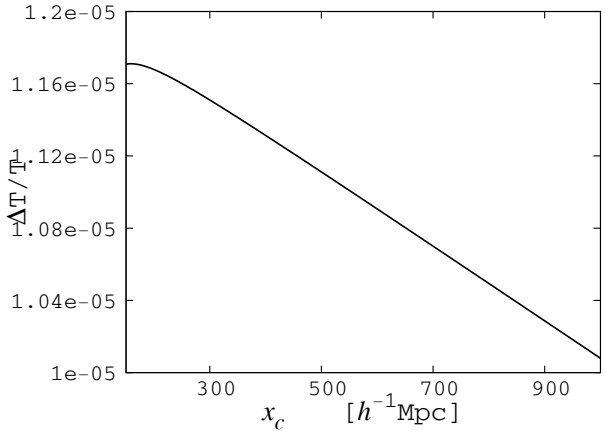

Fig. 3 Relationship between the amplitudes of the local quadrupole and the radius of the local gravitational field for $x_0 = 112\,h^{-1}\,\mathrm{Mpc}$.

Table 2 Power in Quadrupole C_2 and Alignments of the "Foreground-corrected" CMB Maps for ILC1, ILC3 and ILC5

	$C_2\,(\mu\mathrm{K}^2)$	S	$P(S)\,(\%)$
ILC1-corr	1064.2	0.317	75.1
ILC3-corr	1034.2	0.371	61.5
ILC5-corr	1022.3	0.368	62.2
ΛCDM	1071.5	0.412	50.0

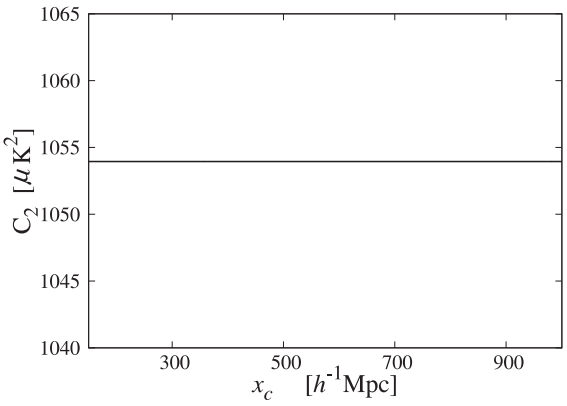

Fig. 4 Corrected C_2 for ILC5, when $x_0 = 112\,h^{-1}\,\mathrm{Mpc}$.

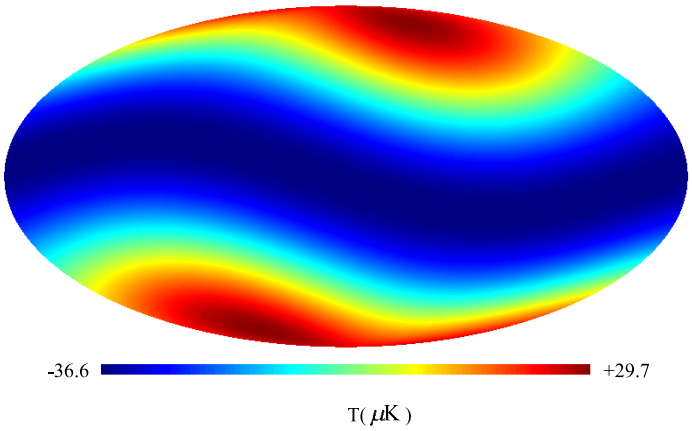

Fig. 5 Local quadrupole map. The direction of the local gravitational field is $(284^\circ, 74^\circ)$, the density fluctuation is 10^{-3}, and it is about $112\,h^{-1}\,\mathrm{Mpc}$ away from us.

We evaluate the probability that the primary quadrupole is cancelled by the local quadrupole. We generate 2000 CMB maps, which have random quadrupole orientations, with the HEALPix software, and the input theoretical power spectra, $C(\ell)$, are generated by the CAMB package. Then, we combine the foreground with the random, statistically isotropic CMB maps. We find that about $\sim 28\%$ of the quadrupole's values are consistent with the observed WMAP five year values, that is $C_2 = 223.479 \pm 978.367$[3]. Therefore, our model can explain part of the anomalies, but the large errorbar in the quadrupole measurement may also be responsible for the large number of 28%.

4 CONCLUSIONS

In this paper, we have re-investigated the anomalies in WMAP data. The power in the quadrupole is found to be $C_2 = 204.4\,\mu\mathrm{K}^2$ for ILC1, $C_2 = 260.3\,\mu\mathrm{K}^2$ for ILC3 and $C_2 = 254.1\,\mu\mathrm{K}^2$ for

[3] *http://lambda.gsfc.nasa.gov/product/map/*

ILC5, while the power in the quadrupole for the standard $\Lambda\mathrm{CDM}$ model is $C_2 = 1071.5\,\mu\mathrm{K}^2$. It is obvious that the power in the quadrupole is less than expected. By comparing the distribution of the S statistics from WMAP data to those from 10^6 MC simulations mimic CMB maps, we found that they are consistent at the level of 0.8% for ILC1, 2.1% for ILC3 and 1.2% for ILC5. These results indicate that the quadrupole and octopole planes are strongly aligned.

We provide a possible explanation for the anomalies in WMAP data by using the foreground model caused by a large density fluctuation. The model depends on the matter distribution, and the position of the observer. So, we assumed that there is a large-scale structure in direction $(284\,^\circ, 74^\circ)$, the center is $\sim 112\,h^{-1}\,\mathrm{Mpc}$ away from us, and the density fluctuation is 10^{-3}. After subtracting the mock foreground caused by such an area from the WMAP data ILC1, ILC3 and ILC5, we found that the power in the quadrupole, C_2, increases to the $(\sim 1000\,\mu\mathrm{K}^2)$ level, and the S decreases to the $0.31 \sim 0.37$ level, which agrees with the prediction from the standard $\Lambda\mathrm{CDM}$ model. To conclude, the local gravitational collapse might be responsible for explaining the origin of the large-angle CMB anisotropy.

Recently, it has been suggested by many researchers that the local inhomogeneities can account for the large angular scale anomalies (Tomita 2005a,b; Vale 2005). However, none of the proposed models can successfully explain the anomalies (Inoue & Silk 2006). This is because it is well known from GR that in a linear approximation, the behavior of a comoving object in an expanding or collapsing metric cannot be equivalently described as SR Doppler motion if the higher orders are involved. The amplitude of the kinematic quadrupole is about 13% of the cosmic quadrupole (Wu & Fang 1994). Therefore, the CMB quadrupole anisotropy calculated as an effect of a local density inhomogeneity cannot be approximated by an SR effect, which is the main reason why we have derived different results from others.

However, many other specific features of the anomalies have been discovered, such as anomalously cold spots on angular scales $\sim 10^\circ$ (Vielva et al. 2004; Cruz et al. 2005), and asymmetry in the large-angle power between opposite hemispheres (Eriksen et al. 2004; Hansen et al. 2004b; Sakai & Inoue 2008). We have not interpreted these anomalies with our model explicitly, so further research is expected.

Acknowledgements We would like to thank Wen Xu, Huan-Yuan Shan, Xiao-Chun Mao, Xin-Juan Yang, Nan Li and Qian Zheng for helpful comments and discussions. In addition, we are grateful to the WMAP team for providing such a superb data set. We also thank Wen Xu for careful reading on the draft manuscript.

References

Abramo, L. R., Sodre, Jr. L., & Wuensche, C. A. 2006, Phys. Rev. D, 74, 083515
Bennett, C. L., Banday, A. J., Gorski, K. M., et al. 1996, ApJ, 464, L1
Bennett, C. L., Hill, R. S., Hinshaw G., et al. 2003, ApJS, 148, 97
Campanelli, L., Cea, P., & Tedesco, L. 2006, PhRvL, 97, 131302
Copi, C. J., Huterer, D., & Starkman, G. D. 2004, Phys. Rev. D, 70, 043515
Copi, C. J., Huterer, D., Schwarz, D. J., et al. 2006, MNRAS, 367, 79
Copi, C. J., Huterer, D., Schwarz, D. J., et al. 2007, PhRvD, 75, 023507
Cruz, M., Martínez-González, E., Vielva, P., et al. 2005, MNRAS, 356, 29
de Oliveira-Costa, A., & Tegmark, M. 2006, Phys. Rev. D, 74, 023005
de Oliveira-Costa, A., Tegmark, M., Zaldarriaga, M., et al. 2004, Phys. Rev. D, 69, 063516
Efstathiou, G. 2004, MNRAS, 348, 885
Eriksen, H., Hansen, F., Banday, A., et al. 2004, ApJ, 605, 14
Finkbeiner, D. P. 2004, ApJ, 614, 186
Gaztañaga, E., Wagg, J., Multamäki, T., et al. 2003, MNRAS, 346, 47

Gordon, C., Hu, W., Huterer, D., et al. 2005, Phys. Rev. D, 72, 103002
Górski, K. M., Hivon, E., Banday, A. J., et al. 2005, ApJ, 622, 759
Hansen, F. K., Balbi, A., Banday, A. J., et al. 2004b, MNRAS, 354, 905
Hansen, F. K., Cabella, P., Marinucci, D., et al. 2004a, ApJ, 607, L67
Hinshaw, G., Nolta, M. R., Bennett, C. L., et al. 2006, ApJS, 170, 288
Hinshaw, G., Weiland, J. L., Hill, R. S., et al. 2009, ApJS, 180, 225
Inoue, K. T., & Silk, J. 2006, ApJ, 648, 23
Inoue, K. T., & Silk, J. 2007, ApJ, 664, 650
Katz, G., & Weeks, J. 2004, Phys. Rev. D, 70, 063527
Kocevski, D. D., & Ebeling, H. 2006, ApJ, 645, 1043
Land, K., & Magueijo, J. 2005, PhRvL, 95, 071301
Lewis, A., Challinor, A., & Lasenby, A. 2000, ApJ, 538, 473
Prunet, S., Uzan, J. P., Bernardeau, F., et al. 2005, Phys. Rev. D, 71, 083508
Rakić, A., Räsänen, S., & Schwarz, D. J. 2006, MNRAS, 369, L27
Sakai, N., & Inoue, K. T. 2008, Phys. Rev. D, 78, 063510
Schwarz, D. J., Starkman, G. D., Huterer, D., et al. 2004, PhRvL, 93, 221301
Spergel, D. N., Verde, L., Peiris, H. V., et al. 2003, ApJ, 148, 175
Spergel, D. N., Bean, R., Doré, O., et al. 2006, ApJS, 170, 377
Tomita, K. 2005a, Phys. Rev. D, 72, 043526
Tomita, K. 2005b, Phys. Rev. D, 72, 103506
Watkins, R., Feldman, H. A., & Hudson, M. J. 2009, MNRAS, 392, 743
Wu, X. P., & Fang, L. Z. 1994, ApJ, 424, 530
Vale, C. 2005, arXiv: astro-ph/0509039
Vielva, P., Martínez-González, E., Barreiro, R. B., et al. 2004, ApJ, 609, 22